

10-24-2004

Immobilization of Fission Iodine by Reaction with a Fullerene Containing Carbon Compound and Insoluble Natural Organic Matrix

Spencer M. Steinberg
University of Nevada, Las Vegas, spencer.steinberg@unlv.edu

Gary Cerefice
University of Nevada, Las Vegas, cerefice@unlv.nevada.edu

David W. Emerson
University of Nevada, Las Vegas

Follow this and additional works at: https://digitalscholarship.unlv.edu/hrc_trp_separations

 Part of the [Analytical Chemistry Commons](#), [Oil, Gas, and Energy Commons](#), and the [Physical Chemistry Commons](#)

Repository Citation

Steinberg, S. M., Cerefice, G., Emerson, D. W. (2004). Immobilization of Fission Iodine by Reaction with a Fullerene Containing Carbon Compound and Insoluble Natural Organic Matrix. 1-28.
Available at: https://digitalscholarship.unlv.edu/hrc_trp_separations/40

This Annual Report is protected by copyright and/or related rights. It has been brought to you by Digital Scholarship@UNLV with permission from the rights-holder(s). You are free to use this Annual Report in any way that is permitted by the copyright and related rights legislation that applies to your use. For other uses you need to obtain permission from the rights-holder(s) directly, unless additional rights are indicated by a Creative Commons license in the record and/or on the work itself.

This Annual Report has been accepted for inclusion in Separations Campaign (TRP) by an authorized administrator of Digital Scholarship@UNLV. For more information, please contact digitalscholarship@unlv.edu.

Project Title:

**Annual Report: Immobilization of Fission Iodine by Reaction with a Fullerene
Containing Carbon Compound and Insoluble Natural Organic Matrix**

October 28, 2004

Principal Investigator: Dr. Spencer M. Steinberg (Chemistry)
4505 S. Maryland Parkway
Las Vegas NV 89154-4003
Phone: 702-895-3599
Email: spencer.steinberg@ccmail.nevada.edu

International Collaborator: **V.G. Khlopin Radium Institute – Research-Industrial
Enterprise (KRI-KIRSI)** St. Petersburg, Russia
Dr. Boris E. Burokov (KRI-KIRSI, PI)
Dr. Michael Savopulo (Co-PI, KRI-KIRSI Director)

Collaborators (UNLV): Dr. David W. Emerson (Co-PI, Chemistry)
Dr. Gary Cerefice (HRC)
Gregory Schmett (Graduate Student, UNLV Chemistry)
Ginger Kimble (Graduate Student, UNLV Chemistry)

AAA Project Collaborator: Dr. James Laidler
Dr. George Vandegrift
Chemical Technology Division, Argonne National
Laboratory

AAA Research Area: Separations

Abstract:

The recovery of iodine released during the processing of used nuclear fuel poses a significant challenge to the transmutation of radioactive iodine. During the first two years of this program we have examined the potential of Fullerene Containing Carbon compounds (FCC) developed by KRI, and natural organic matter (NOM) as sorbents for iodine released during the reprocessing of nuclear fuel. This work involved the development of bench-scale testing of the FCC and NOM material in a simulated process off-gas environment.

Research Objectives and Goals

- Develop bench-scale experimental set-up and procedures for simulating PUREX head-end vapor phase; Develop experimental procedures for evaluating I sequestering methods using bench scale procedures.
- Develop FCC-bearing material as potential I sequestration matrix.
- Determine binding of iodine to FCC and NOM.
- Examine alternate I sequestration matrices using techniques developed for FCC and NOM studies.
- Examine the effect of reaction conditions on binding.
- Elucidate the nature of the reaction products (volatile, hydrophobic, soluble, insoluble). See Figure 1 for example.
- Develop methodology and host matrix for converting sequestered I to solid matrix for evaluation as transmutation target and/or disposal matrix.
- Examine recovery of I from sequestration matrices using combustion, hydrolysis and pyrolysis methods.

Scope: The recovery of iodine released during the processing of used nuclear fuel poses a significant challenge to the transmutation of radioactive iodine. This project examines the use of Fullerene Containing Carbon (FCC) compounds as potential sorbents for iodine release from the reprocessing of nuclear fuel. This work will also include the development of bench-scale testing capabilities at UNLV to allow the testing of the FCC material in a simulated process off-gas environment. This experimental capability will also be used to test other potential sorption materials and processes, such as natural organic matter (NOM) and other promising alternatives. This work will also examine the development of a process to convert the sorbed iodine into a ceramic material with the potential for use as either a transmutation target or as a waste form in a partitioning and sequestration strategy.

Bench scale experimental apparatus and methodologies to simulate iodine entrainment in the vapor phase released from the head end of the PUREX process (the nitric acid dissolution of spent nuclear fuel) were developed, along with procedures to test the sequestration of iodine from the vapor mixture. Long-term performance/suitability of FCC and NOM will be tested for sequestration of iodine released by nuclear fuel

reprocessing. FCC-bearing materials will be prepared and evaluated under laboratory conditions by KRI-KIRSI. Simulated process evaluations were done on the FCC-bearing materials, NOM, and other matrices suggested by the collaborators at UNLV. Conversion of the sequestered iodine to a ceramic-like material will be examined by the KRI-KIRSI team. Recovery of the iodine from the sequestering matrices will also be examined (by both teams).

Analytical Methods:

The development of analytical methods for measuring the speciation of iodine after reaction of iodine and iodate with sphagnum is continuing. We have continued to use pyrolysis to examine iodine release from NOM. We have continued the experiments with iodinated sphagnum peat and have quantified the amount of iodine released as methyl iodide during pyrolysis. We have developed a method for calibrating the GC/MS for methyl iodide. Gaseous methyl iodide standards are prepared by injecting neat methyl iodide into glass gas sampling bottles that had been previously purged with nitrogen. An aliquot of the standards (10 μL) was removed with a gas sampling syringe and injected into a small quartz tube filled with approximately 10 mg of Carbosphere™ (a carbon molecular sieve). This standard (in Carbosphere) was processed using the pyrolysis method described in previous reports. Desorption from the Carbosphere was accomplished by ballistic heating to 500 °C using the Pyroprobe 2000 instrument described in previous reports. Methyl iodide was quantified by monitoring the 142 (m/e) peak on the chromatogram. An example calibration is presented in figure 1.

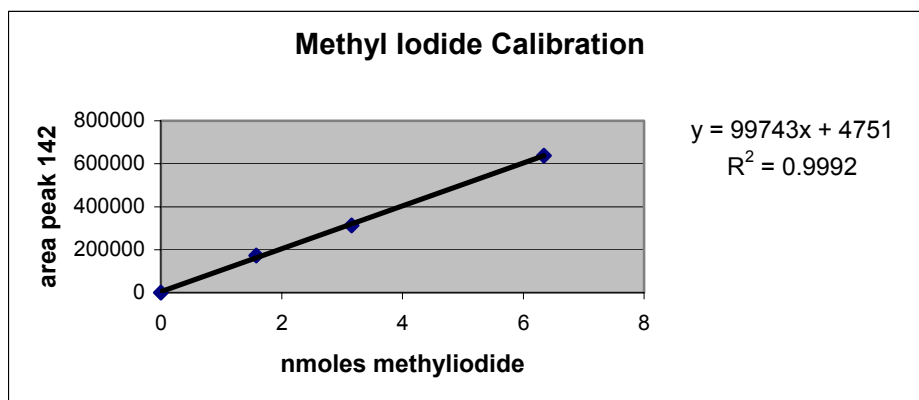


Figure 1: Example calibration for methyl iodide.

We are employing this pyrolysis method for examining the release of methyl iodide from several anion exchange resins, in addition to the sphagnum peat. These results will be discussed further below.

We have extended the use of iodine trapping (as p-iodo-N,N-dimethylaniline, I-NNDMA) as a way of quantifying remaining iodine in studies with both model compounds and sphagnum. We have performed some time series experiments to examine the reaction rate of iodine with several model compounds and with sphagnum.

In Figure 2 a time series is shown for the reaction of vanillin with iodine at pH 2.5. The pH in this experiment was controlled with a phosphate buffer. Remaining iodine in this solution was quantified with the NNDMA procedure outlined above. The initial iodine concentration was 82 μM . The graph indicates that the reaction proceeded very rapidly, although the iodine concentration reached a finite plateau rather than decreasing to zero (undetectable). This is probably an artifact of the low pH and the limited capacity of the buffer to control additional protons released by the aromatic substitution. The maximum iodide that could be released if the reaction proceeded as a reduction is also shown. These results indicate that half of the iodine atoms are released as iodide while the remainder became associated with the vanillin ring. Note that even at low pH the reaction kinetics are rapid and difficult to follow.

Vanillin Reaction with Iodine pH 2.5

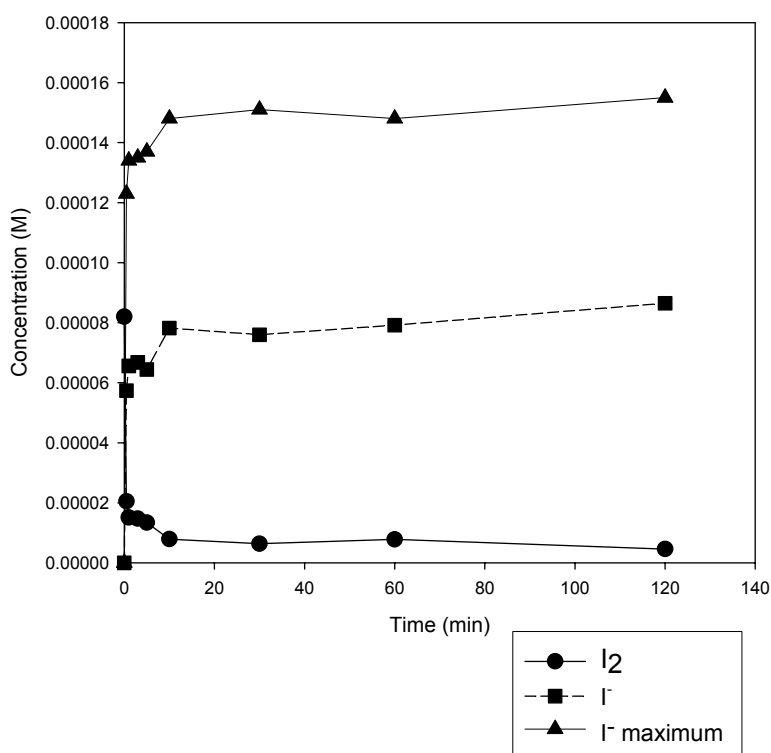


Figure 2: Reaction of iodine with vanillin (40 μM) at 25 $^\circ\text{C}$ and pH 2.5.

Again the iodide detected (and plotted in Figure 2) by ion chromatography was corrected for the iodide released by the reaction of NNDMA with iodine remaining in the solution.

Reaction of Iodine with Sphagnum in Aqueous Suspension:

We studied the I_2 reaction kinetics with sphagnum peat and other types of natural organic matter (NOM) as a function of pH. In these studies the NNDMA method was used to quantify iodine remaining in solution. Our measurements indicate that the reaction of

iodine with organic matter results in carbon iodine bond formation (binding) as well as reduction of the iodine to iodide. We performed a series of time series measurements that enable us to propose a mechanism. A series of sphagnum buffer suspensions was prepared. The reaction was started with the addition of a known quantity of iodine. After a measured period of time the reaction was terminated by the addition of NNDMA. The NNDMA and I-NNDMA were extracted from the suspension with hexane and measured by GC/MS. The “solid” organic mater was removed by filtration and iodide was analyzed in the aqueous phase. This procedure is illustrated in Figure 3.

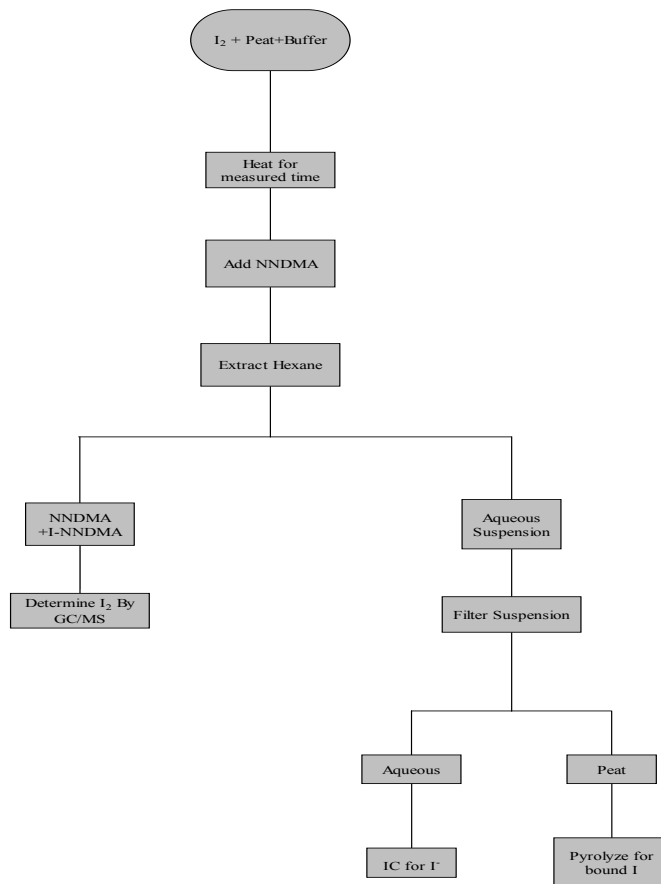


Figure 3: The processing of sphagnum buffer suspensions used to investigate the kinetics of the reaction with iodine.

We have obtained additional data on the reaction of peat with iodine at pH 2, 6, 8, 10. As will be discussed below, the data indicates a pseudo first order reaction of iodine with peat. A plot illustrating the disappearance of iodine (as $\ln [I_2]$ vs. time) is shown below in Figure 4. The reaction rate at pH 10 was too fast to follow by our method.

I₂ and Peat

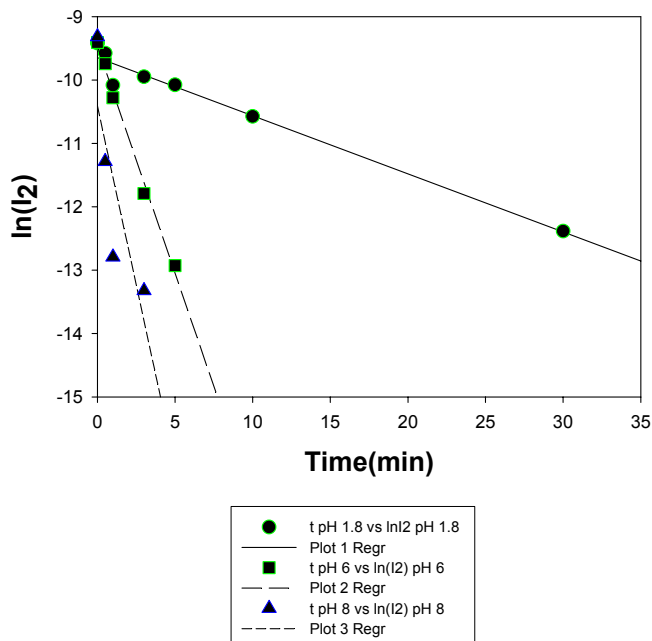


Figure 4: Apparent first order reaction of iodine with Sphagnum peat in aqueous suspension.

The reaction of iodine (I₂) with a suspension of Sphagnum Peat (350 mg/10 mL of Buffer) appears to be pseudo first order in I₂. The pH dependence of the pseudo first order rate constant (k_t) is illustrated in Figure 5. The reaction at pH 10 was also studied but was too fast to follow by our method. The rate constant at pH 10 was estimated from a single data point. This apparent first order rate constant represents the sum of the reduction and peat addition (ring addition) reactions.

log k_t vs. pH

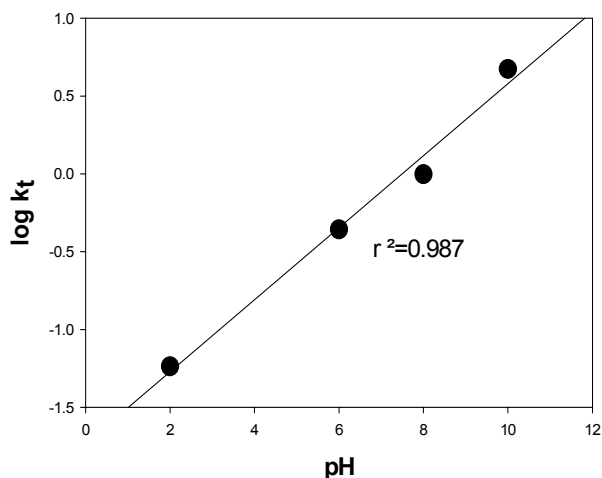
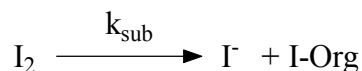
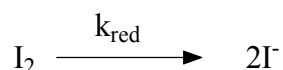


Figure 5: The pseudo first order rate constant for iodine binding as function of pH.

Table 1: Pseudo first order rate constants (min^{-1}) for reaction of iodine with sphagnum peat (350 mg/10 mL buffer). Rate constants were estimated by linear regression of $\ln(I_2)$ against time.

pH	k_t	% Ring Substitution
2	0.058	--
4.7	0.26	100
5.8	0.44	100
8	1.0	55
10	4.7	40

The loss of iodine and the appearance of iodide (in the presence of excess sphagnum) can be modeled using the simple reaction scheme (P represents the reactive Sphagnum).



Reaction Scheme 1: The reaction of iodine with excess sphagnum peat. I-org is represents iodine bound to the peat matrix (phenolic rings?).

This reaction scheme can be represented as two parallel first order equations.

$$\frac{dI_2}{dt} = -(k_{\text{red}} + k_{\text{sub}}) * I_2 \quad \text{Equation 1}$$

$$\frac{dI^-}{dt} = 2 * k_{\text{red}} * I_2 + k_{\text{sub}} * I_2 \quad \text{Equation 2}$$

The rate constant k_{red} and k_{sub} are pseudo first order rate constants for the reduction of iodine and substitution of iodine for hydrogen on the organic matrix (ring substitution?). The concentrations of I_2 and I^- are plotted as a function of reaction time in Figure 6 for pH 5.8. The two differential equations presented above have been fit to the data using a numerical method (Bulirsch-Stoer Integrator). Fitting was accomplished using a commercial software package (Scientist™ from Micromath). The lines in Figure 6 represent an example of the least square fit results. The reaction of iodine with sphagnum proceeds partially by reduction and partially by reaction of iodine with the organic material resulting in a substitution of iodine for hydrogen. The top horizontal line represents the iodide concentrations for complete reduction. The bottom horizontal line represents the predicted iodide concentration for ring substitution.

Peat pH 5.8 I₂ Kinetics

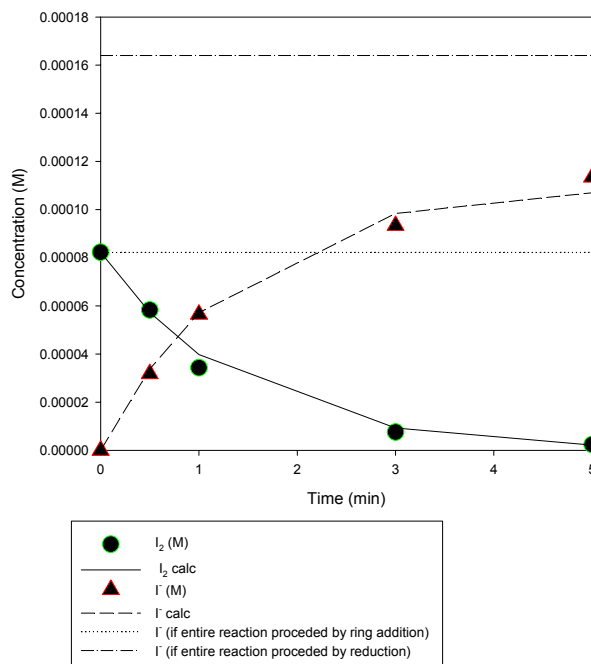


Figure 6: Iodine and Iodine concentrations as a function of time the presence of a suspension of Sphagnum peat (at pH 5.8). The lines represent best-fit results.

The best-fit values for the rate constants for several pHs are as follows. We were not able to fit the data for pH 2 because iodide could not be determined by ion chromatography. The ion selective electrode values were not accurate enough for fitting purposes. Similarly the pH 10 data only had a single point and could not be fit.

Table 2: Best fit values for the rate constant obtained by fitting Figure 6 to equations 1 and 2.

pH	k_{red} (min ⁻¹)	k_{sub} (min ⁻¹)	k_t (min ⁻¹)	% Ring
4.7	~0	0.63	0.63	100
5.8	0.25	0.48	0.73	66
8	0.41	0.61	1.02	60

The fraction of iodine that reacts by substitution can be calculated from the rate constants:

$$\% \text{Substitution} = \frac{100 * k_{\text{sub}}}{k_{\text{sub}} + k_{\text{red}}} \quad \text{Equation 3}$$

The results of this calculation, along with the calculated k_t are shown in Table 2. About 66% of the iodine reacted by “ring substitution” at pH 5.8, and 60% at pH 8.

The fit of the time series data to equation 1 and 2 yield rate constants for ring substitution and reduction. The sum of these two process should be close to the the pseudo first order rate constant k_t for the loss of iodine that was presented in Table 1. Comparison shows only qualitative agreement with the k_t (Table 1). The differences in the values are caused by the need to simultaneously fit two equations in the numerical fitting of equations 1 and 2, and in the differences in weighting of data points between the two types of statistical approaches. Iodide mass balances in these experiments indicate that ring substitution is the dominant reaction.

Fractionation of the peat, and iodide-iodine mass balance demonstrate that iodine atoms are becoming associated with the insoluble organic material during these experiments. The incorporation of iodine was verified by pyrolysis of the recovered (and air dried) peat. Pyrolysis at 400 – 600°C releases iodine as methyl iodide.

We utilized these heating experiments to determine if soluble organic iodine compounds were formed by reaction of peat and iodine. In order to address the formation of volatile and semi-volatile iodo-compounds we have exposed NOM solutions to iodine (at several pHs) and then fractionated the mixture as shown below (Figure 7).

The aqueous phases from these reaction mixtures were examined for semi-volatile species. The aqueous phase was passed through a solid phase extraction (C_{18}) cartridge. Semi-volatile compounds retained by the solid phase cartridge were derivatized with BSTFA (silation agent) and examined by GC/MS. Our previous observations indicate only minute formation of iodoform and other volatile iodinated alkanes were formed. Similarly, we were not able to detect the formation of any semi-volatile iodinated organic compounds under these conditions.

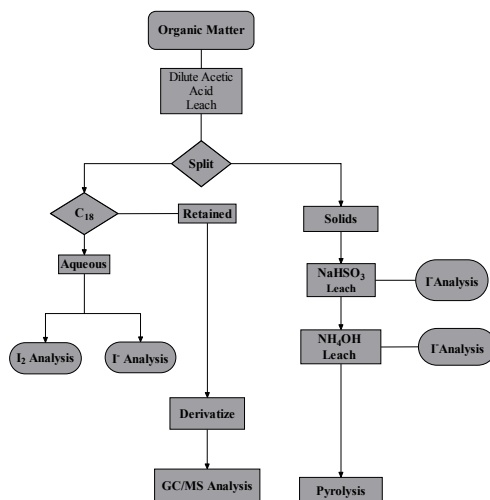


Figure 7: NOM/I₂ fractionation assessing the formation of volatile and soluble iodinated compounds.

The solid material remaining in the reaction mixture was leached with several reagents (ammonia and bisulfite) to determine the amount of iodine easily removed by hydrolysis or nucleophilic displacement. The solid was dried and subjected to pyrolysis and the amount of iodine released as methyl iodide was quantified. The amount of methyl iodide produced by pyrolysis was 5-8% and appeared independent of pH in the range of 4-12. A second series of experiments was conducted where 0.5 g of unbuffered sphagnum was treated with 1.5 to 6.0 mL of 250 ppm iodine. After 24 hours of exposure the samples were dried and pyrolyzed *without the leaching procedure outline above*. The results indicated that on average 40% of the applied iodine was converted to methyl iodide. There was no indication of iodine dose dependence in the methyl iodide yield in these experiments, which was certainly surprising. However, the methyl iodide formed was 20-25 times the apparent blank levels and so unambiguously related to the treatment. It may be that sampling of the treated sphagnum selected for iodinated “hot spot” because of textural changes induced by treatment. In other words iodine rich particles of sphagnum may be selectively sampled, for pyrolysis, because of differences in texture and density induced by the treatment. We are investigating this possibility. Grinding of the remaining peat with mortar and pestle does improve reproducibility of the results.

Reaction of sphagnum peat with iodate:

During the first year of this study it became apparent that iodine could be oxidized to iodate in the presence of nitric acid and nitrogen dioxide. Therefore, we have conducted a large number of experiments to determine the possible reaction of iodate with sphagnum peat moss. These experiments indicate that the natural organic material reacts with iodate and result in the formation of bound iodine (organo iodine) and/or iodide. This reaction is much slower than iodine reaction. For this reason we studied the reaction at 60°C. Heating experiments (up to 12 hour) were conducted over a range of pHs. Experiments (pH buffered) were conducted with 350 mg of Sphagnum peat in 10 mL of 57 µM iodate. It is clear from these results that much of the iodate is reduced to iodide. Experiments at pH of 2-9 and demonstrated that 5-30% of the iodine (from the iodate) is incorporated into the peat. The incorporation of iodine from iodate has been quantified by pyrolysis GC/MS. We have quantified the amount of iodine released as methyl iodide during pyrolysis (Figure 8). In addition, we have measured the concentration of residual iodate and iodide produced by the treatment (Figure 9).

Methyl Iodide Yield from Peat Iodate Heating Experiments

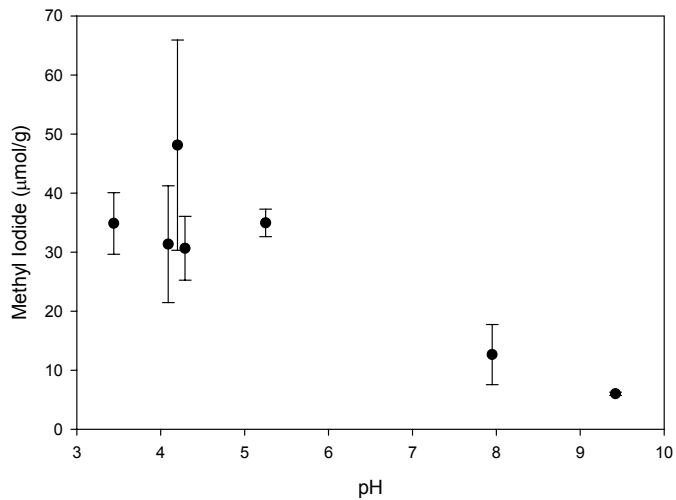


Figure 8: Methyl iodide generation from iodate treated peat (12 hours at 60°C).

Iodate Reaction with Peat 60°C 12 Hours

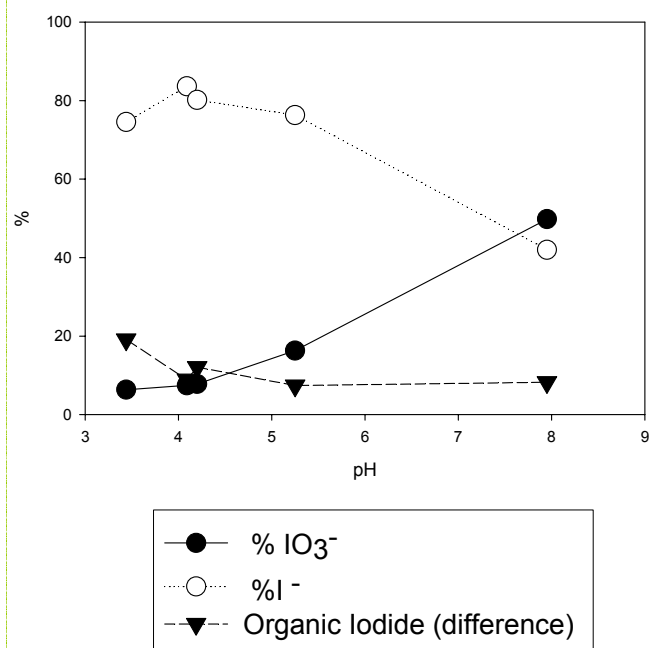


Figure 9: The amount of iodate and iodide in peat suspensions after 12 hours of heating. The amount of organic iodine was calculated by difference.

The kinetics of this process is illustrated in Figures 10-11. The reaction of iodate follows pseudo first-order kinetics. Iodide is formed by reduction of iodate in addition to organically bound iodine. The organically bound iodine appears to go through a maximum with reaction time indicating that it is eventually released into the solution as iodide. The loss of iodate follows pseudo first order kinetics. As shown in Figure 13, the reaction rates of peat with iodate decreases with increasing pH. We interpret this trend as an indication of increasing electrostatic repulsion between the peat matrix and the iodate with increasing pH. The increase in pH causes increasing negative charge as a result of the ionization of carboxylic acid and phenolic functional groups. The reaction rate of iodate is about one order of magnitude slower than that of iodine. We have obtained some preliminary data that indicates that iodate is first converted to hypoiodic acid (HOI), which in turn, can be further reduced to iodide, or react with peat resulting in sequestration into the organic matrix. This reaction presumably occurs as a substitution for hydrogen at phenolic rings. The reaction of iodate with peat appears to involve competition (parallel reactions) between sequestration and reduction to iodide. We are working on a model for this process.

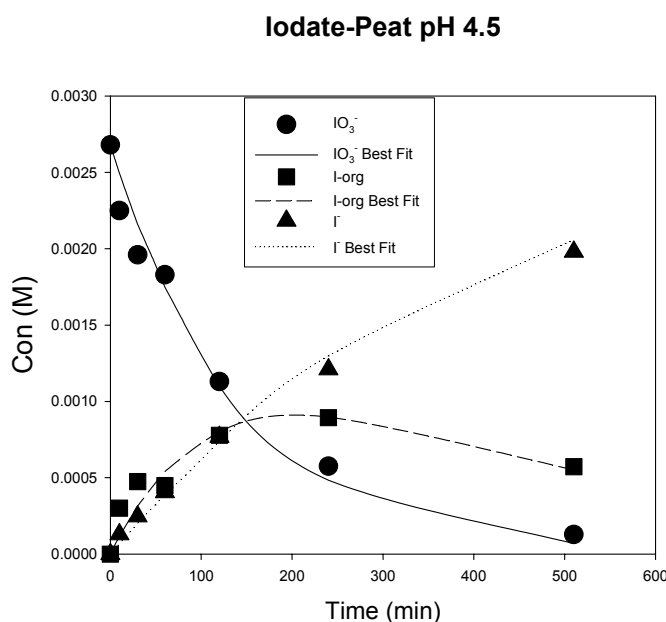


Figure 10: Reaction of IO_3^- with sphagnum peat at 60°C at pH 4.5. I-org corresponds to the organic bound iodine (substitution) and was calculated by mass balance. Iodate and iodide were measured by ion chromatography.

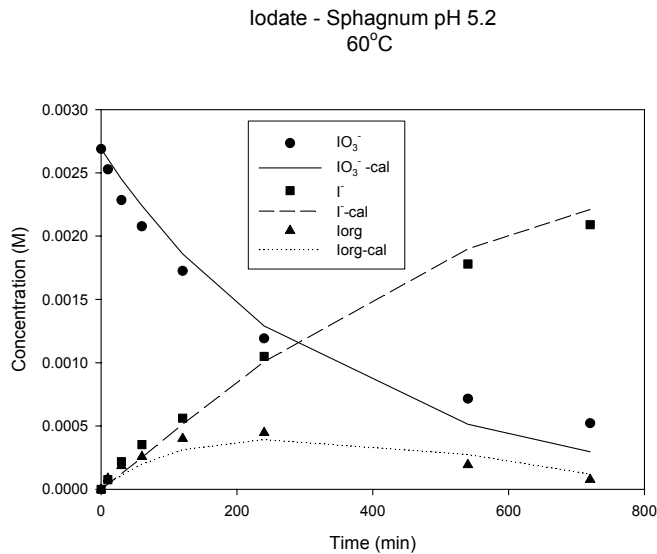


Figure 11: Reaction of IO_3^- with sphagnum peat at 60°C at pH 5.2. I-org corresponds to the organic bound iodine (substitution) and was calculated by mass balance. Iodate and iodide were measured by ion chromatography.

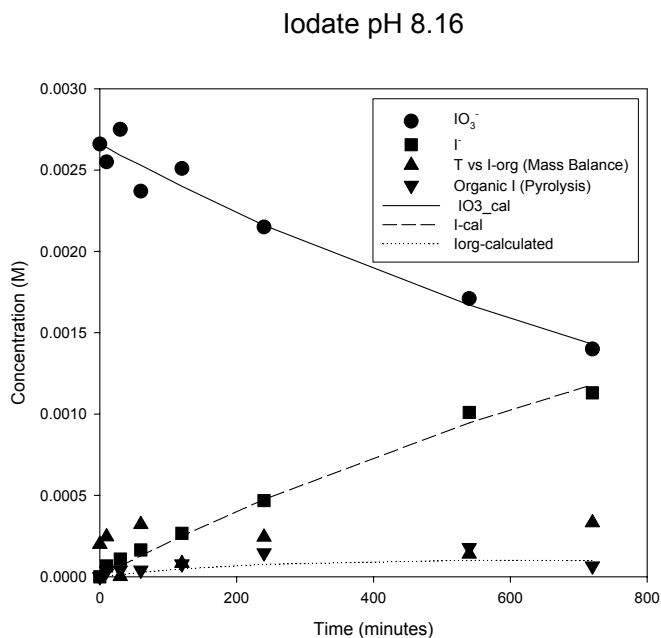


Figure 12: Reaction of IO_3^- with sphagnum peat at 60°C at pH 8.16. I-org corresponds to the organic bound iodine (substitution) and was calculated by mass balance. Iodate and iodide were measured by ion chromatography.

logk vs. pH

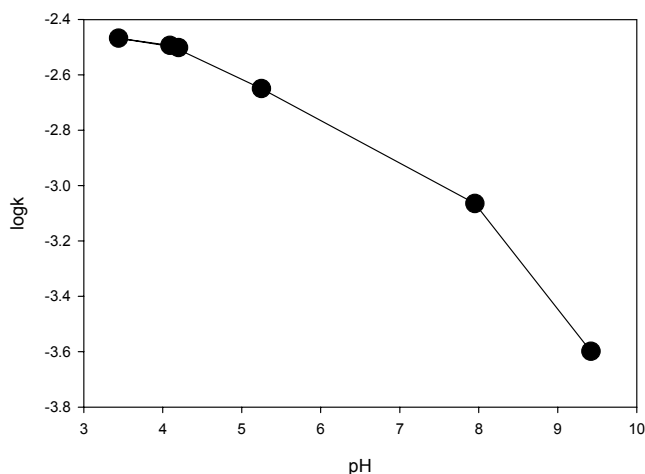
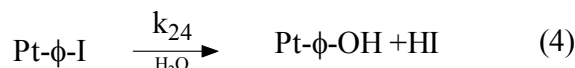


Figure 13: The pseudo first order rate constants for loss of iodate at various pHs at 60°C.

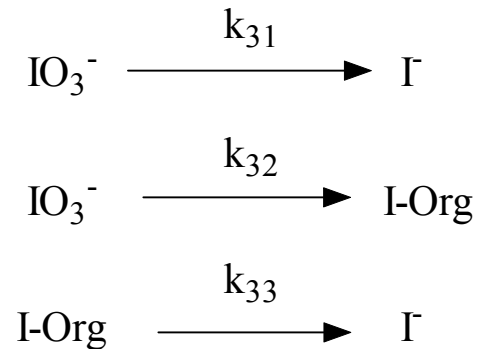
We believe that this pseudo first order loss of iodate during these experiments represent two parallel reaction (both proceeding from the IOH intermediate). In one reaction IOH is reduced to iodide, the second reaction results in attack on a phenolic moiety in the peat. The IOH intermediate is formed as a result of the sphagnum peat's inherent reducing capacity. This reduction capacity may result from reactive functionalities such as aldehydes and hydroquinone groups. We gave summarized this hypothesis in reaction scheme 2, where the first line (1) represents the reduction of iodate to IOH by the sphagnum. We believe these reductive steps are rate determining in the process. The second reaction (2) represents reduction of IOH (an intermediate) to iodide. The third reaction (3) is a competitive substitution reaction, where by the iodine (from IOH) becomes incorporated into an aromatic moiety in the sphagnum structure. At the temperature (60°C) that these experiments were conducted the sphagnum bound iodine was not stable. This is indicated by reaction 4, which represents hydrolysis (base mediated?) of the aromatic iodide functionality.



Reaction Scheme 1: Proposed model for reduction of iodate and incorporation of iodine into sphagnum peat. Pt represents the peat mediated processes k_{ij} are pseudo first order rate constants for each step. Pt=peat. Pt- ϕ -H is an aromatic ring with an available H. Pt- ϕ -I is the substitution product.

This proposed mechanism is certainly not proven, but we believe that it is consistent with the data that have been obtained. We have been able to trap the IOH intermediate with a competitive reaction, and the indications are that trapping IOH reduces the incorporation of iodine into the sphagnum. We are conducting additional measurements to verify these observations.

We have modeled the evolution of iodine species in these experiments using the following simplified reaction scheme:



Reaction Scheme 2: Simplified reaction scheme for iodate with sphagnum peat.

Three pseudo first order reactions were assumed. The relationship between the rate constants in reactions schemes 2 and the rate constants in the simplified scheme 3 can be established by making a steady state approximation on IOH in scheme 2. The rate constants k_{31} and k_{32} correspond to the rate of formation of IOH in scheme 2, multiplied by the fraction of the IOH that proceeds by reduction and substitution respectively.

For example:

$$k_{31} = \frac{k_{21}k_{22}}{k_{22} + k_{23}} \quad \text{Equation 4}$$

$$k_{32} = \frac{k_{21}k_{23}}{k_{22} + k_{23}} \quad \text{Equation 5}$$

The constant k_{33} is the same as k_{24} . We have utilized numerical fitting of Figures 10-12 to estimate the above rate constants.

Table 3: Rate constants (min^{-1}) estimated, using numerical methods, for reaction scheme 3.

pH	k_{31}	k_{32}	k_{33}
4.55	2.69E-03	4.44E-03	2.70E-03
5.17	1.50E-03	1.54E-03	4.68E-03
8.16	7.20E-04	1.93E-04	2.65E-03

The pH dependence of the rate constant is illustrated in Figure 14. The apparent reduction of iodate to iodide and the formation of organic iodide decrease with pH. The hydrolysis of the organic iodide does not show a significant pH trend.

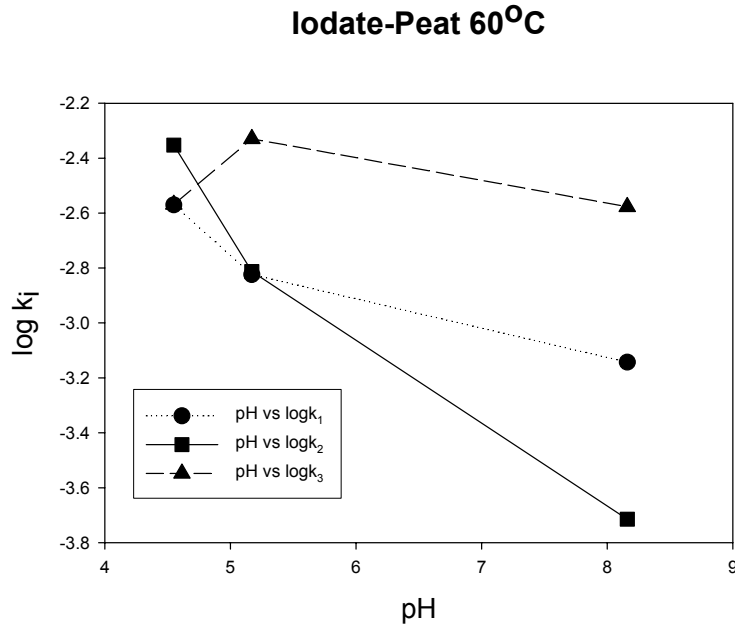


Figure 14: pH dependence of best-fit rate constants

For both iodine and iodate experiments we have verified the incorporation of iodine into sphagnum peat using the pyrolysis technique. Pyrolysis of sphagnum peat (at 500°C) from either type of experiment results in the release of methyl iodide.

The formation of iodide from iodine during fuel rod dissolution would result in reduced fugitive iodine during fuel dissolution. However this iodide is also water soluble and highly mobile in the environment. We are exploring the potential use of ion exchange resins for temporarily sequestering this iodide.

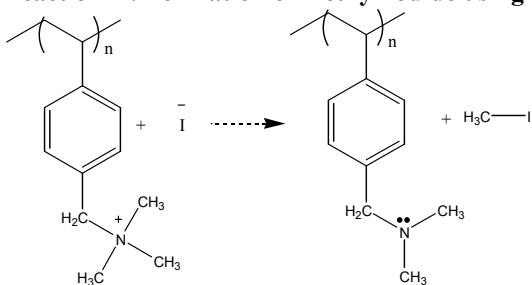
Resin studies:

We believe that iodate can ultimately be reduced to iodide by NOM. Iodide can be extracted (removed) from aqueous solutions with strongly basic ion exchange resins. Strongly basic ion exchange resins possess tetra-alkyl ammonium ion exchange sites. Hydrophobic anions such as iodide have a high affinity for these sites. Experiments were performed using ion exchange resins to sequester iodide. One line pursued consisted of studying the affinity of various ion exchange resins for iodide ions in potassium iodide solutions. The resins that showed some potential were of the quaternary ammonium type (AG-1 and AG-641). AG-1 retained 1.38 milliequivalents of iodide per g (meq/g) of resin and A-641 retained 2.03 meq/g. Eluting the iodide from AG-1 proved difficult. Solutions containing both sodium chloride and sodium perchlorate were required for recovery of iodide.

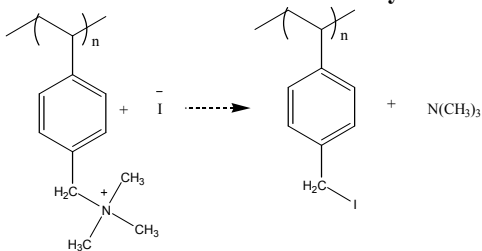
To recover iodine from these anion exchange resins one can take advantage of the strongly nucleophilic nature of iodide. Previous studies have demonstrated that quaternary ammonium ions are susceptible to nucleophilic displacement reactions. Thermal decomposition of the iodide salts of alkyltrimethylammonium surfactants produces alkyl dimethylamines. In the case of benzyl trimethyl ammonium cations, nucleophilic attack by iodide results in the formation of either benzyl iodide or methyl iodide.

We performed some pyrolysis experiments with several different anion exchange resins. The first resin was AG-1 x8. This is a standard commercially anion exchange resin that is normally available commercially in the chloride form. This resin was treated with excess iodide (KI) in preparation for the pyrolysis study. The second resin investigated for this type of application is a methyl-pyridinium type resin. This resin was made from a commercially available polyvinyl-pyridine resin (Reillex HP). Reacting methyl iodide with the polyvinyl-pyridine starting material formed the iodide salt of methyl-pyridinium. Vacuum dried (over NaOH) specimens of both resins were analyzed by pyrolysis GC/MS. The pyrolysis analysis was performed on a Varian Saturn III GC/MS equipped with a CDS Pyroprobe 2000. Several resin beads were packed into a small diameter quartz tube and held in place by quartz wool. The beads were generally heated to 300-500C for 20 seconds. The pyrolysis products are swept from the quartz tube onto the GC column with the helium carrier gas. One loop of the column was immersed in liquid nitrogen to focus (cryo) the off-gas onto the column. Heating experiments with the iodide form of the strongly basic AG-1 resin indicated that heating produced either methyl iodide (Reaction 2) or trimethyl amine (Reaction 3).

Reaction 2: Formation of methyl iodide using AG-1 resin.



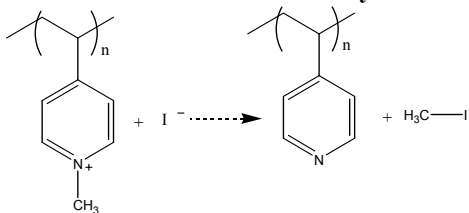
Reaction 3: Formation of trimethylamine from AG-1 resin



Heating experiments with the methyl pyridinium resin produced methyl iodide. The

reaction we propose is shown in reaction 4. With mixed iodide and chloride salts of the methyl pyridinium resin both methyl iodide and methyl chloride were observed.

Reaction 4: Formation of methyl iodide from methyl pyridinium resin.



Results with AG1-X8 indicate that reaction 3 occurs preferentially at 300° C while at 500°C methyl iodide production (reaction 2) dominates. A series of pyrolysis experiments was performed on iodine saturated AG-1 X8. The ratio of methyl iodide to trimethyl amine was measured as a function of temperature. Samples (0.5-1 mg) were heated for 20 seconds and the pyrolysis gases analyzed by GC/MS. The ratios reported are the integrated ratios from the total ion chromatograms. These results are summarized in Figure 15, which illustrates that formation of methyl iodide dominates the resin decomposition at higher temperatures.

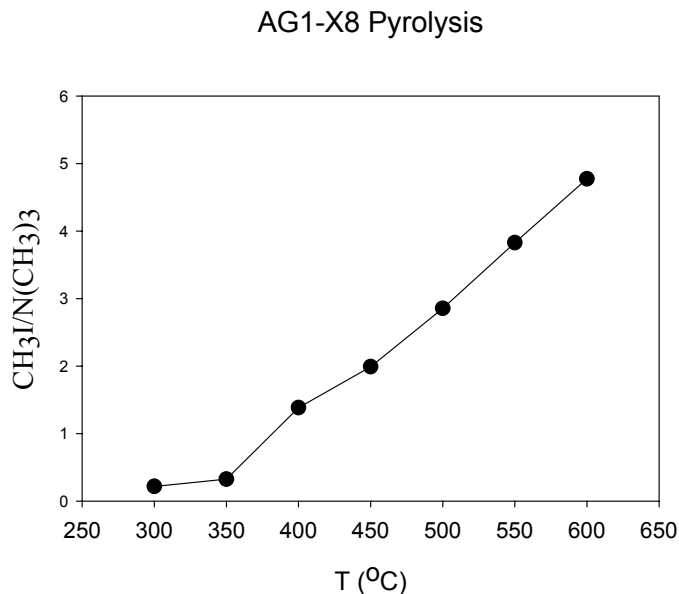


Figure 15: The ratio of methyl iodide and to trimethyl amine as a function of pyrolysis temperature.

AG1-X8 Pyrolysis

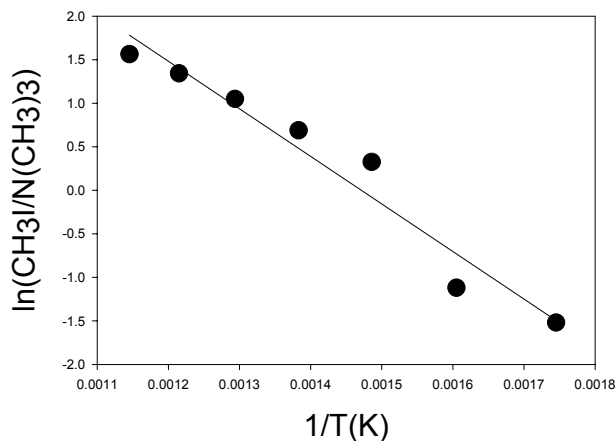


Figure 16: The change in predominant resin decomposition mechanism as a function of temperature is a result of difference in activation energy for the competing reactions.

Methyl iodide formed during this process can be recovered for further processing. Pyrolysis of the dried resin and produced methyl iodide, while pyrolysis of the starting material produced trimethyl amine and small amount of methyl chloride. Therefore, one of the tasks involved in exploring this approach will be to determine a temperature suitable for high recovery of methyl iodide while minimizing the formation of other cracking products.

Preliminary experiments with methyl pyridinium resin in the iodide form produced methyl iodide upon heating. Preliminary experiments indicated a maximum production of methyl iodide at 450 °C (Figure 17).

Methyl Pyridinium Resin

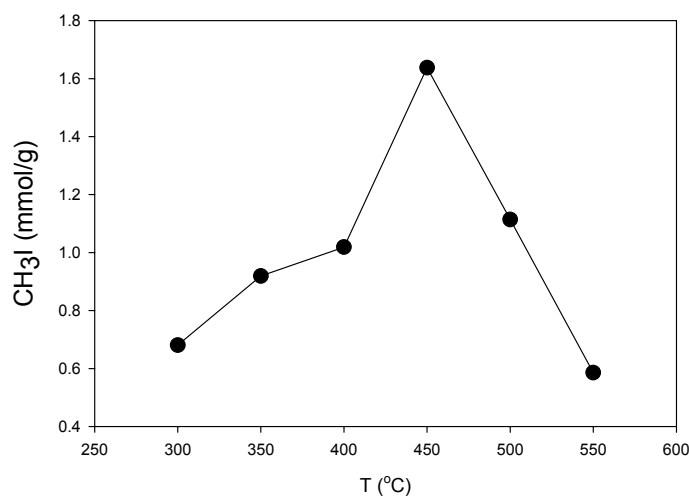


Figure 17: The production of methyl iodide by pyrolysis of methyl pyridinium resin maximizes at a pyrolysis temperature of 450°C.

We anticipate the methyl iodide produced by heating of the anion exchange resin can be concentrated cryogenically or by adsorption on carbon, or carbon molecular sieve. Methyl iodide can then be converted into a target material for transmutation.

Some preliminary studies have also been performed with a phenyl dimethyl sulfonium anion exchange resin. The sulfonium functionality behaves in a similar fashion as the quaternary ammonium functionality that was discussed above. The iodinated form of this resin also produced methyl iodide upon heating. The competitive reaction is the release of dimethyl sulfide. Early results show that the release of dimethyl sulfide predominates at higher temperatures (Figures 18,19).

Phenyl dimethyl Sulfonium Pyrolysis

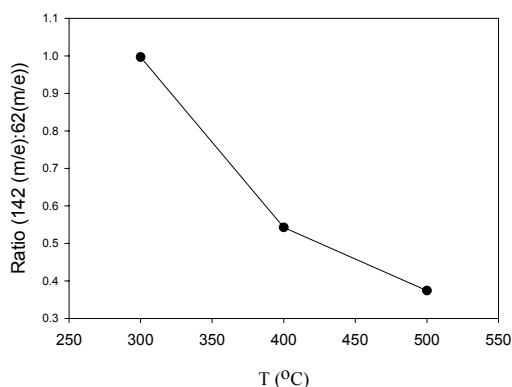


Figure 18: The production of methyl iodide (mass 142) decreases with increasing temperature, in favor of the production of dimethyl sulfide (mass 62).

Phenyl dimethyl Sulfonium Pyrolysis

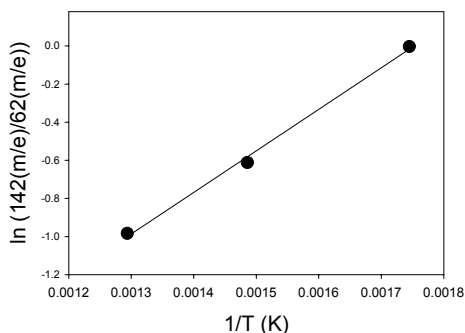


Figure 19: Changes in the production of methyl iodide with temperature are a result in the higher activation energy for formation of dimethyl sulfide. This is analogous to the quaternary ammonium type resin discussed above.

During the next contract year we will be exploring the recovery of methyl iodide from sphagnum peat and from ion exchange resins. We will develop a technique for converting

methyl iodide to NaI. We have ordered the equipment necessary to begin the next phase of experiments.

The trapping of methyl iodide produced during pyrolysis is another possible role for reactive resin. As noted above, iodine trapping experiments showed that when natural organic matter (NOM) was used to trap iodine, pyrolysis of the NOM released a substantial amount of methyl iodide. We experimented briefly with trapping methyl iodide on a resin having an ethylselenyl ($\text{CH}_3\text{CH}_2\text{-Se}\sim$, $\text{EtSe}\sim$) functional group that should react readily with the $\text{EtSe}\sim$ group to form $\text{P}\sim\text{Se}(\text{Et})(\text{Me})^+\text{I}^-$. A simple experiment to test this was carried out by placing 0.3 g of the resin in a bottle, introducing either 20 or 40 μL of methyl iodide, capping the bottle with a septum cap, and sampling the head space for MeI after a period of time. No solvent was used. With both sample sizes, 58% of the methyl iodide was removed by the resin. Pyrolysis of the resin produced both methyl and ethyl iodide as anticipated (Umemura et al., *Bull. Chem. Soc. Jpn.* **1990**, *63*, 2593-2600) showing that $\text{P}\sim\text{Se}(\text{Et})(\text{Me})^+\text{I}^-$ was formed. This finding is important because if it becomes necessary to trap methyl iodide (containing ^{129}I) it can likely be done using a resin $\text{P}\sim\text{SMe}$ that will form $\text{P}\sim\text{S}(\text{Me})_2^+ ^{129}\text{I}^-$. It should then be possible to treat this sulfonium salt, $\text{P}\sim\text{S}(\text{Me})_2^+ ^{129}\text{I}^-$, with sodium hydroxide to form $\text{P}\sim\text{SMe}$, methanol, and sodium iodide thus regenerating the trapping agent $\text{P}\sim\text{SMe}$ and producing a water solution of Na^{129}I , and volatile methanol.

Iodine Vapor Trapping Experiments:

We have conducted additional experiments with the iodine generator and the fuel rod dissolution simulator in order to examine the effects of nitric acid fumes and NO_2 (at 40°C) on iodine sequestration. Previously we demonstrated that our NOM traps, prepared with sphagnum peat and $\text{Ca}(\text{OH})_2$, were able to trap iodine vapor in the presence of nitric acid vapor. Only a small fraction of the iodine was released by water as iodide or iodate (<10%). If the main reaction was addition of iodine to the aromatic ring a stoichiometric amount of iodide should be produced (1:1). Furthermore, this iodide should be leachable from the column. In the absence of nitric acid fumes less than 15% of the adsorbed iodine was desorbed from the column with water. This is significantly less than the 50% we would predict if addition to aromatic rings were the primary reaction. It is interesting to compare this result with the reaction of a suspension of sphagnum moss with an aqueous solution of iodine. At pHs of greater than 10 (with prolonged heating) most of the iodine was apparently reduced to iodide. Experiments with the fuel rod dissolution simulator indicate that both FCC and NOM are capable of trapping iodine.

We have done additional experiments with the iodine generator and measured breakthrough curves for different ratios of peat to $\text{Ca}(\text{OH})_2$. In Figure 1 we illustrate the effect of $\text{Ca}(\text{OH})_2$: sphagnum ratio on iodine sorption by natural organic matter. These experiments are conducted with our iodine generator device at iodine concentrations of about $\sim 10^{-5}$ mol/L in the presence of nitric acid fumes. In all of these experiments, the traps were packed with about 0.5 g of the sphagnum and $\text{Ca}(\text{OH})_2$ mixture. The results

indicate that the 30% $\text{Ca}(\text{OH})_2$ mixture was most effective for sequestering iodine under these conditions.

Our results (Figure 19) indicate that $\text{Ca}(\text{OH})_2$ at 10% and 60% was less effective than 30%. We believe that the role of the base is two fold. First, the hydroxide deprotonates phenolic moieties making the peat more reactive toward iodine. Second, the hydroxide promotes the disproportionation of iodine, which immobilizes fugitive iodine. Disproportionation, may slow the reaction of iodine with the peat by trapping iodine in a less reactive form.

Iodine Breakthrough Variable $\text{Ca}(\text{OH})_2$
Flow rate 20.0 mL/min, 0.46 g trap

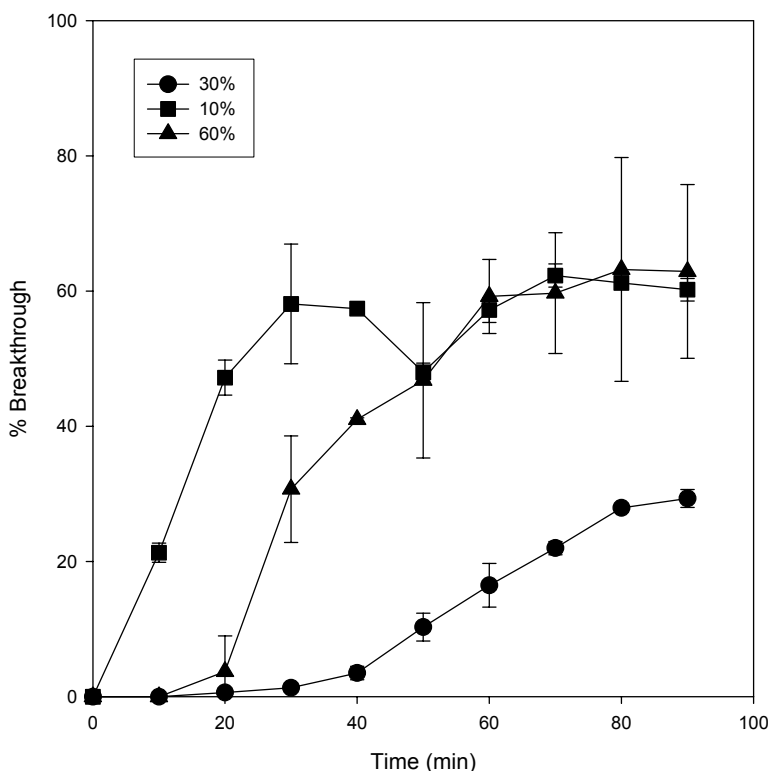


Figure 20: Percent iodine breakthrough for three different Sphagnum Peat/ $\text{Ca}(\text{OH})_2$ ratios. The trap consisted of ~ 0.5 g of $\text{Ca}(\text{OH})_2$: sphagnum mixtures. Three ratios were tested: 10, 30, 60%. The flow rates were 20.0 mL/min and the concentration of iodine was $\sim 10^{-5}$ mol/L. The carrier was 50% saturated with nitric acid vapor. The breakthrough is shown as a function of pore volumes. Pore volumes were estimated by water displacement. The procedure was reported in earlier reports. 40 min corresponds to approximately 1000 pore volumes.

Our previous results indicate that the generation of NO_2 by the addition of copper metal has some important consequences for iodine speciation. NO_2 oxidized trapped iodine on

the FCC material to IO_3^- . The iodate was easily leached from the column by a water wash (and detected by ion chromatography). Rinsing the column with KI resulted in the generation of an stoichiometrically equivalent quantity of I_2 . Significant iodate was also produced by the NOM under these reaction conditions (reaction 5).



The formation of iodate has important implications for iodide binding by FCC material. NO_2 generation also complicates the determination of breakthrough volumes for iodine in the fuel rod dissolution simulator. Our first group of experiments was done with 0.5 grams of Cu metal. Under these conditions, NO_2 gas fills the reaction vessel and reacts with the bisulfite trapping solution. This limits the time available for monitoring breakthrough. In addition, the NO_x oxidizes iodine that has been previously trapped by the bisulfite.

We have examined the transfer of iodide (in the form of KI) in the fuel rod simulator experiments. We believe that iodide released from fuel rods could be transferred from the sparging vessel as HI or some other volatile form of iodine. Since we wanted to focus on the possible volatile forms of iodine created from KI and nitric acid, these experiments were conducted without out a solid phase absorbent. Iodine transfer was quantified by examining the composition of the bisulfite trapping solution. One possibility is that I^- could be oxidized to I_2 by the nitric acid, which would subsequently be sparged from the system. Other possible volatile forms of iodide are NOI (nitrosyl iodide) which we believe may be formed under these conditions. Several experiment were conducted with KI and nitric acid. Transfer rates were generally less than 25 % over 90 minutes of sparging. In the presence of NO_2 (Cu experiments) I^- was oxidized to iodate (in the reaction vessel). As noted above, NO_2 carried over to the trapping solution depleted the bisulfate concentration. After one experiment conducted with 8 mg of KI, 500 mg of Cu in 25 mL of concentrated nitric acid, it was noted that the bisulfite trap took on a iodine like color. The trap solution reacted positively to KI starch paper indicated that I_2 was probably present in the solution. In order to confirm the presence of iodine we added N,N-dimethyl aniline. This compound reacts quickly with molecular iodine to form 4-iodo-N,N-dimethyl aniline. The solution was extracted and complete iodination was confirmed by GC/MS. The same experiment was conducted in the absence of copper. Without the NO_2 generation active iodine was not observed in the bisulfite trap. Apparently the NO_x acts to deplete bisulfite and oxidize any iodide present to a “reactive” form (I_2 , IOH, NOI). NO_2 likely contributes to oxidation of iodine on FCC and NOM traps as well.

We thoroughly investigated iodine recovery from the first versions of the “fuel rod simulator”. These studies indicate that a significant fraction of iodine (~50%) is lost from the systems. Some of the lose can be explained by the formation of iodate which is absorbed onto the glass surfaces however other losses are ascribed to reaction or absorption of the iodine onto silicone greased surfaces or plastic seals. The fuel rod simulator was rebuilt for the next set of experiments. The redesign eliminated the active surfaces. The new parts and have eliminated greased fittings from the apparatus. With the

exception of the trap material iodine contacts only glass and Teflon. We have demonstrated high recovery of iodine from this system. We have repeated simulated fuel rod dissolution experiments with a trap consisting of 0.02 grams of 70:30 Sphagnum Peat/ $\text{Ca}(\text{OH})_2$. The results of these experiments are shown in Figure 21. Iodine (6 mg) was added to 55mL of 60% concentrated nitric acid. Sparging was started immediately. The amount of iodine remaining in the simulator was determined colorimetrically. The percent of the iodine removed from the system that escaped the trap was recorded as a function of sparging time. The results are presented as a graph of percent iodine against sparging time and trap bed volumes (Figure 19). No significant breakthrough was observed up to 20,000 bed volumes. Higher trapping efficiency could be obtained with a larger trap. The 0.02 grams of material also allowed for easy flow rate adjustments.

Iodine Breakthrough Fuel Rod Simulator
(Glass and Teflon)

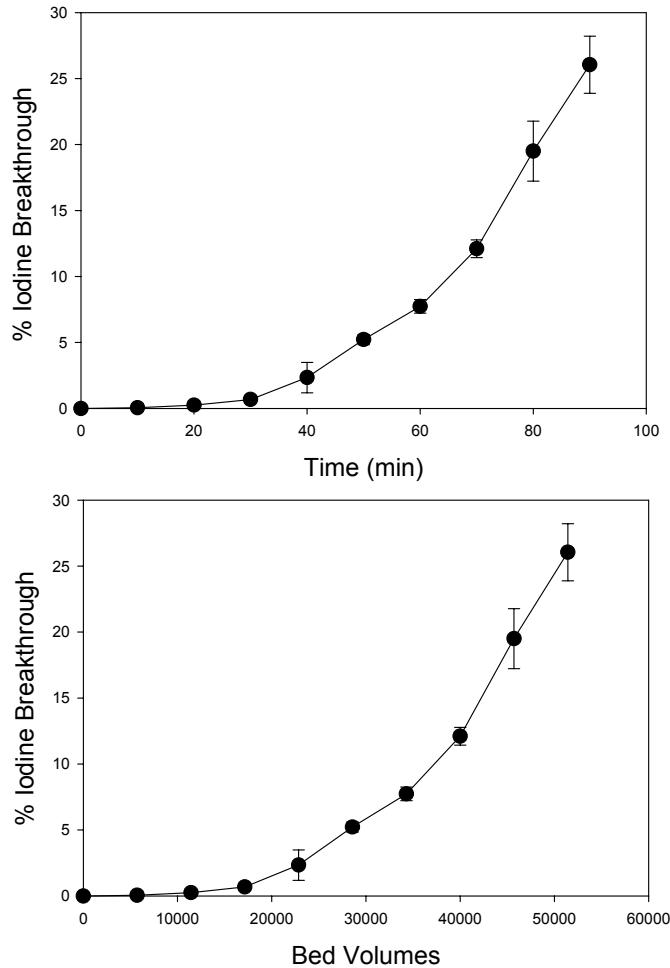


Figure 21: Fuel Rod Simulator Iodine Breakthrough for 0.01 grams of 70:30 Sphagnum/ $\text{Ca}(\text{OH})_2$ and a flow rate of 20 mL/min.

We also tested the effect of varying the $\text{Ca}(\text{OH})_2$ on the reconstructed fuel rod dissolution simulating device. Results for various $\text{Ca}(\text{OH})_2$ /sphagnum ratios are shown in Figure 22 and indicate that the 30% mixture resulted in the smallest breakthrough. These experiments were conducted with very small quantities of sorbent (0.02 g) so that breakthrough could be observed in a reasonable amount of time. With larger amounts of packing material (~0.5 g) breakthrough would not be observed under these conditions.

Fuel Rod Simulator Results

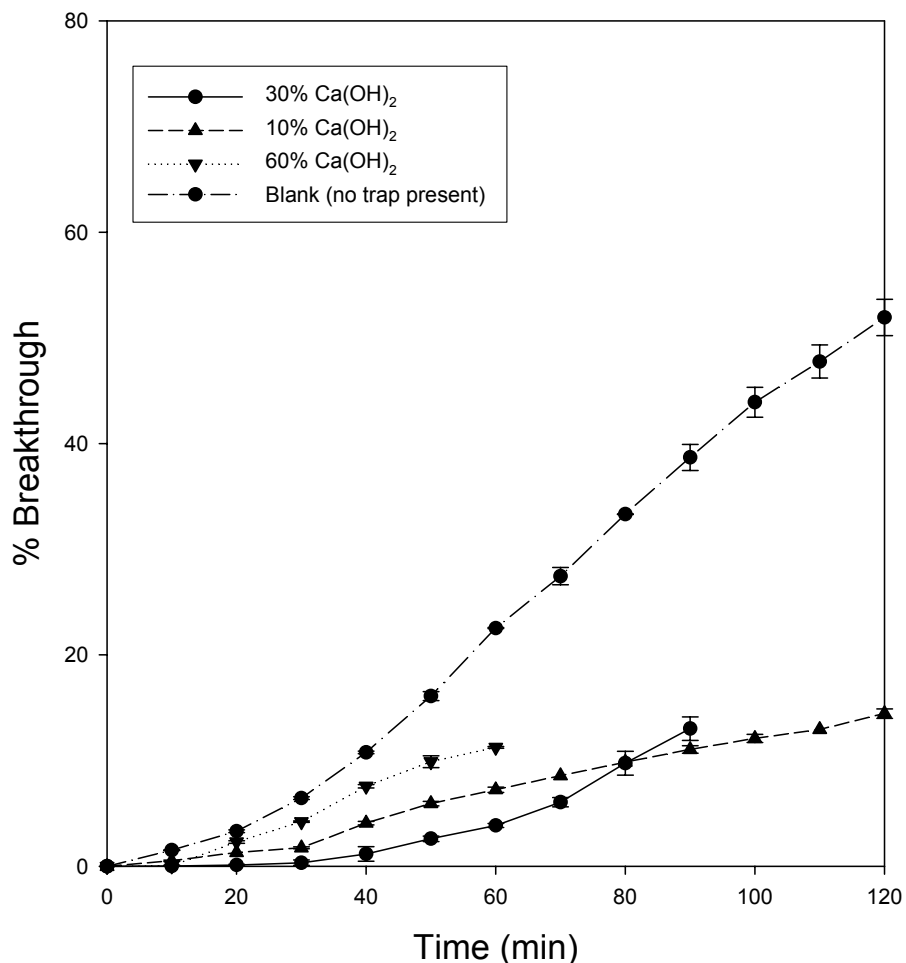


Figure 22: Effect of $\text{Ca}(\text{OH})_2$ content on the efficiency of sphagnum during fuel rod dissolution simulations. All traps contained 0.02g of the sphagnum – $\text{Ca}(\text{OH})_2$ combination.

The NO_2 experiments were repeated with the new system. In these experiments less Cu was used (0.01 g) and had several effects. Both NO_2 and nitric acid are capable of oxidizing iodide. This may occur in the reaction vessel during the dissolution of fuel rods

or after transfer of iodine to the FCC or NOM trap. The formation of highly water-soluble iodate would compromise the sequestration of iodine by either material.

We have tested the effect of NO_2 on the breakthrough of iodine from sphagnum/ $\text{Ca}(\text{OH})_2$ traps. The results obtained with the redesigned fuel rod simulator are illustrated in Figure 23. The presence of NO_2 definitely reduced the breakthrough time (or volume) of the iodine on this type of trap. Because of pressure surges experienced after addition of metallic Cu the breakthrough time was actually faster than “blank” (no trap) experiments.

Fuel Rod Simulation 30% $\text{Ca}(\text{OH})_2$ 70% Sphagnum with NO_2

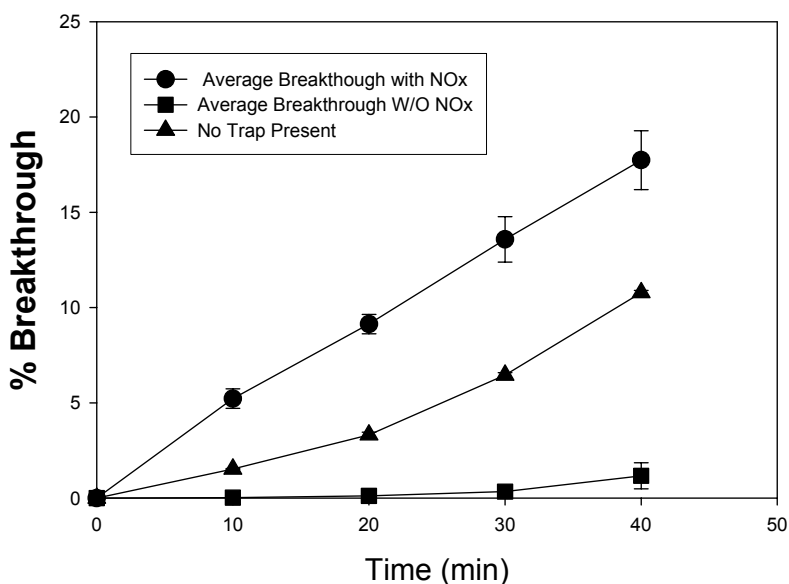


Figure 23: Impact of NO_2 on iodine breakthrough with sphagnum traps using the fuel rod dissolution apparatus.

Similarly the effect of NO_2 on the breakthrough of iodine on the FCC material was studied using the fuel rod simulator apparatus. The results of this study are shown below in Figure 24. Like the sphagnum trap the presence of NO_2 decreases the breakthrough time (or volume) for iodine.

At this stage it is not clear how NO_2 decreases breakthrough. As noted above the addition of Cu (0.01 g) causes a pressure surge in the system. We do not believe this is the complete explanation of enhanced transport. One possibility is the conversion of iodine to another volatile species (INO_2 or INO ?) that is not adsorbed on either FCC or sphagnum. This breakthrough problem could be minimized on the sphagnum by increasing the size of the trap.

FCC Effect of NO₂ on Breakthrough Fuel Rod Simulation

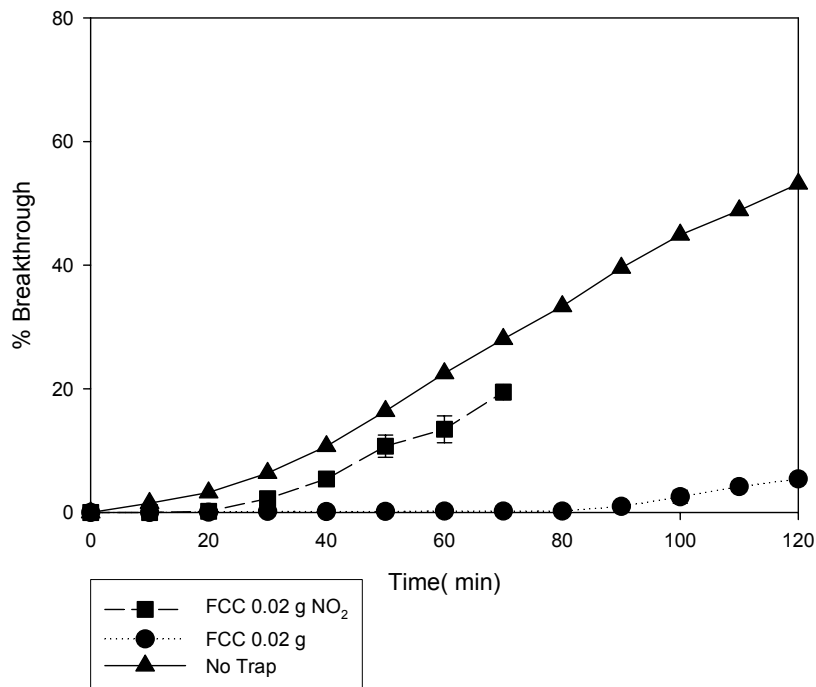


Figure 24: The impact of NO₂ on iodine breakthrough on FCC using the fuel rod dissolution apparatus.

From the work we have concluded so far we believe that iodine reacts with the NOM/Ca(OH)₂ by several mechanism.

1. Ring addition reactions
2. Reduction to iodide
3. Disproportionation in strong alkali (Ca(OH)₂)

We believe that FCC adsorbs iodine as molecular iodine and thermal or chemical adsorption from this material is facile. This is supported by thermal gravimetric measurements of iodine release from FCC-iodine prepared by collaborators at Khlopin. The iodine release occurred at ~200°C, which corresponds roughly to the boiling point of iodine. We believe that FCC acts mainly by physical adsorption, however the sorbed iodine may be converted to iodate (or other species) by HNO₃ or by NO₂.